GEOPHYSICAL RESEARCH LETTERS, VOL. 27, NO. 13, PAGES 1847-1850, JULY 1, 2000

Kinetic Properties of Bursty Bulk Flow Events

Li-Jen Chen,[1,2] G. K. Parks,[2] M. McCarthy,[2] D. Larson,[3] R. P. Lin[3]

Abstract. Particle distributions of bursty bulk flow (BBF) events in the central plasma sheet regions show that the high earthward mean velocity comes from a combination of energetic ion flux increases (>few keV) in the earthward direction and decreases of similar energy fluxes in the tailward direction. The energetic ion increases are observed to ∼few MeV during intense events, indicating the responsible mechanisms efficiently accelerate particles. The BBF events are intimately tied to the dynamics of tail current sheet reconfiguration and for the two events discussed here, they occurred 45 minutes and 5 minutes after the expansion onsets. The perception offered by our analysis differs from the earlier studies which described BBF events using MHD approach.

Introduction

The outer edge of the plasma sheet boundary layer (PSBL) in the geomagnetic tail is permeated with intense ion beams propagating along the magnetic field direction (Forbes et al., 1981; Takahashi and Hones, 1988). These ion beams contribute to high velocity moments (>400 km/s) in the earthward direction. Recent observations show that the PSBL also supports unidirectional ion beams propagating in the tailward direction (Parks et al., 1998). These tailward propagating beams are as intense as earthward propagating beams, but their velocity moments are usually small (<200 km/s). Examination of detailed phase space distributions has clarified why this is so. Whereas the plasma distribution of ion beams propagating in the earthward direction is dominated by the beam component, the tailward beam is superposed on another isotropic component, and the combination of the two distributions yields a small mean velocity in the tailward direction (Parks et al., 1998).

Studies that use plasma bulk parameters consider three variables, the density ($\int f(x,v)d^3v$, where $f(x,v)$ is the particle distribution function), mean velocity ($\int f(x,v)vd^3v$) and mean square velocity ($\int f(x,v)(v_i - \langle v\rangle)(v_j - \langle v\rangle)d^3v$). These parameters are obtained from the reduction of the distribution function. To study the physics beyond that provided by these macroscopic variables, the phase space distributions must be examined. A case in point concerns the counter streaming beams of nearly equal intensities at similar speeds that would yield zero mean velocity moment and a false temperature. The bulk parameter studies miss the presence of these beams. However, a considerable amount of information is contained in these beams that can help our understanding of geomagnetic tail dynamics.

[1]Physics Department, University of Washington, Seattle, WA
[2]Geophysics Program, University of Washington, Seattle, WA
[3]Space Science Laboratory, University of California, Berkeley, CA

Copyright 2000 by the American Geophysical Union.

Paper number 1999GL000009.
0094-8276/00/1999GL000009$05.00

We have thus extended our studies of the phase space distributions of ions and electrons to the vicinity of the central plasma sheet (CPS). The first results established the CPS region often includes multicomponent plasma distributions including ion and electron beams that likely originate from the current sheet (Chen et al., 2000). We have now extended our studies to identify features of plasma distributions that are responsible for high mean velocities in the CPS region. This article will show that the high mean velocities which were identified as bursty bulk flow events (Angelopoulos et al., 1997 and references therein) come mainly from the directional anisotropy of high energy ions (>few keV) which extend to MeV energies during intense events.

Observations

The plasma observations of March 27, 1996 are used to illustrate many of the common features of BBF events that have been observed by the 3D plasma instrument (Lin et al., 1995) on the Wind spacecraft during its first 25 perigee passes through the near-earth CPS region of the geomagnetic tail. The top three panels of Figure 1 summarize the first three moments of the distribution function obtained by the electrostatic analyzer (PESA-HIGH) during the time interval 10-15 UT (the second moment has been interpreted as temperature for purposes of comparison but it does not necessarily have an equilibrium meaning as defined in thermodynamics especially when the distribution is multicomponent). The fourth panel shows the three components of the magnetic field (courtesy of R. Lepping). The bottom two panels are energy spectrograms for fluxes travelling in the sunward and tailward directions. The time resolution of ion measurements is 48s or 24 s and of the magnetic field, 3s. The GSM position of the Wind spacecraft at 1030 UT was $(-14.8, 12.0, 1.3)$ and at 1430 UT $(-15.6, 6.8, 1.1)$ in Earth radii (R_e).

The velocity moments show several events with $\langle V_x\rangle$ that exceed 400 km/s in the earthward direction (second panel). But note that there is also significant $\langle V_y\rangle$. These events have typical durations of ∼10 minutes and the concurrent magnetic field measurements made on Wind indicate signatures of the CPS region ($B_{xy} < 15nT$, or $B_z/B_{xy} > 0.5$, criteria used by Angelopoulos et al., 1992), except for the event at 1410 UT, which was accompanied by >20 nT $|B_x|$ and a density ∼0.1/cc, indicating properties of the PSBL. These high earthward $\langle V_x\rangle$ events are associated with B_z increases and have been studied by Angelopoulos et al. (1997) who identified them as BBF events.

The sunward energy spectrogram indicates that ion flux increases that contribute to the high $\langle V_x\rangle$ events have typical energies of ∼ 10 keV. An important feature about these events is that significant sunward flux increases are detected to the highest energy channel of the detector (∼27 keV). At the same time, tailward fluxes decrease from the highest energy channels down to a few keV. This combination of

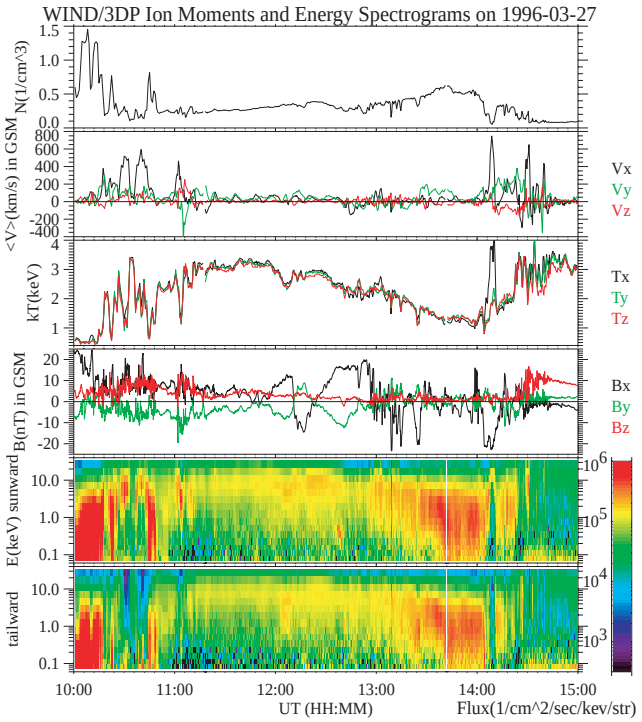

Figure 1. The top three panels show the first three computed moments of the ion distribution function for March 27, 1996. The fourth panel shows the three components of the magnetic field. The bottom two panels show energy-time spectrograms of ions travelling in the sunward and tailward directions.

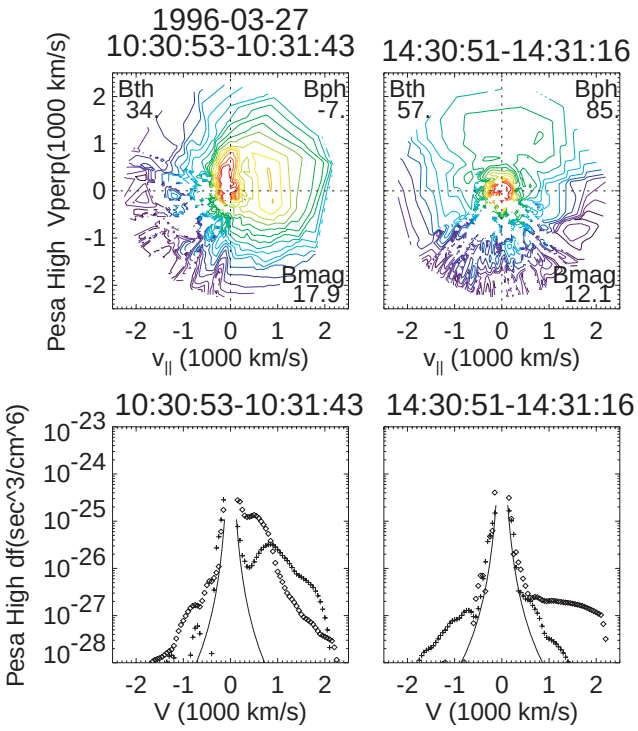

Figure 2. Isocontours of phase space density and 1D cuts of the ion distributions in$(V_{\parallel}, V_{\perp})$ space for the two BBF events (see text for details).

flux increase and decrease of high energy ions in the two opposite directions is the main cause for the high velocity moments.

Figure 2 shows examples of ion distributions for the events that occurred around 1030 and 1430 UT. These plots, in the spacecraft frame, represent 2D slices of the 3D distributions along the plane whose normal is defined by $\mathbf{B}\times\mathbf{V}$, where $\mathbf{V}$ is the mean velocity, with $\hat{B}$ as X-axis and $\hat{V}_{\perp}$ as Y-axis. The lines are isocontours of phase space densities in $(V_{\parallel}, V_{\perp})$ space. The magnetic elevation (Bth) and the azimuth (Bph) angles are shown on the top right and left and the intensity on the lower right. The corresponding 1D cuts of the distributions are shown in the bottom row. Both cuts along (+) and perpendicular ($\diamondsuit$) to the magnetic field are plotted to illustrate the behavior of the low energy and the high energy components while the solid line denotes the instrument background level. The ion distribution for the 1030 UT event (48 s average) includes a core of anisotropic low energy ions that is elongated along $V_{\perp}$ and is slightly shifted in the antiparallel direction, and a broad beam covering $\sim 45^{\circ}$ in pitch-angles along the magnetic field direction at ~900 km/s, ~5 keV. Both the core and the energetic beam are displaced from the origin by ~200 km/s along $+V_{\perp}$, indicating the plasmas at this time were being convected by $E\times B$ drift based on its velocity-independent nature. The 1430 UT distribution (24 s average) shows an extremely hot component that lies along the $V_{\perp}$ direction. The corresponding perpendicular 1D cut shows a sharp break at ~500 km/s, above which is a plateau that extends out of the scale, and below it is a soft component that extends to the lowest threshold of our detector.

The increase of high energy ion flux extends to the 2.082 MeV channel of the solid state telescopes (SST) as shown in Figure 3, which is a stack plot of omnidirectional ion fluxes of various energies from both the electrostatic analyzer (PESA-H) and SSTs. Figure 4 shows examples of energy spectra from ~70 eV to a few MeV taken before, during and after the 1030 and 1430 UT events. Spectra from 120 angular bins are displayed for PESA-H and 44 for SST. The directions are color-sorted to reveal information on the direction along which the ions are travelling. The red/black and purple are toward the Sun and the green is antisunward.

The first spectrum is taken from ~1000 UT. There are low and high energy components present in the spectrum. The SST shows continuation of the high energy component. We will focus primarily on the directional behavior of the high energy component. Note for the 0959:54 spectra, before the event, there is little spread indicating the ions are isotropic. For the 1430 UT event, ions from few keV to 2 MeV all display similar directional anisotropy, with sunward flux (red and black) the highest and antisunward (green) the lowest. Similar anisotropy extends from a few keV to 1 MeV for the 1030 UT event. The spreading of these spectra demonstrates that the fluxes at any given energy are highly dependent on direction. The 1450:57 spectra, after the events, show isotropy similar to the spectra before the event, but with larger intensities of energetic particles. Finally, note that the peak of the 1430 UT spectrum lies at the high end of the energy detection threshold (~30 keV) for PESA-H. This incomplete sampling of the ion population indicates the moments calculated from the PESA-H ion distribution underrepresents the actual values of the real population.

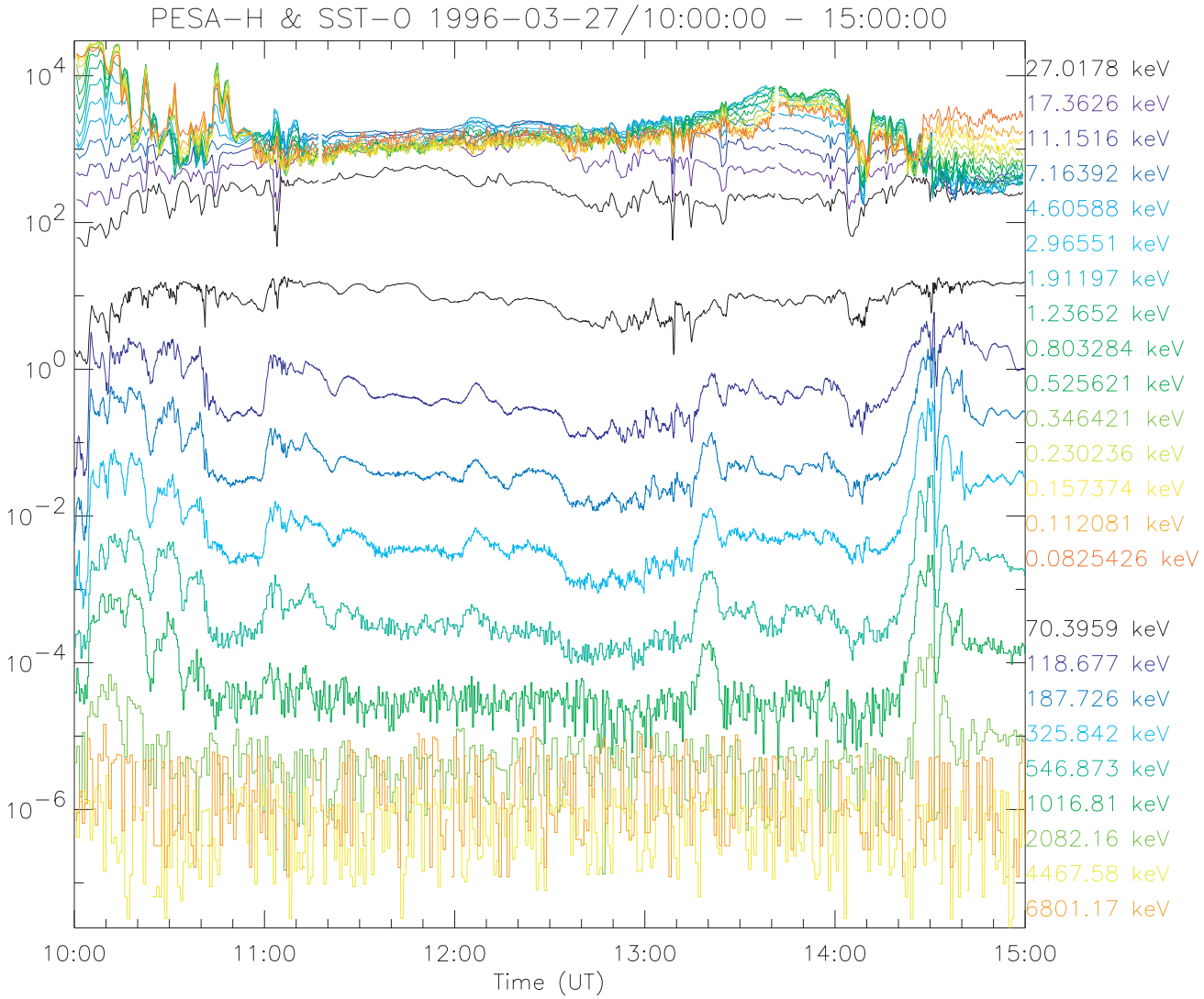

Figure 3. Stack plots of ion fluxes from ∼70 eV to 6.8 MeV. Note the increase of ion fluxes in the 2 MeV channel at 1430 UT during the BBF event.

Summary and Discussion

The events we report in this article are the same events studied previously by Angelopoulos et al. (1997) who used MHD approach to characterize the BBFs. The extension of the analysis into the kinetic domain has led to widely different conclusions. The first concerns the interpretation of the increase of the second moment in terms of ion heating associated with BBFs. As we have shown in Figure 1, 3, and 4, this increase comes from the addition of energetic ions, instead of a broadening in velocity space of the original population (heating). The second concerns the large velocity moments which have been interpreted as $E \times B$ convective flows (Angelopoulos et al., 1996). Our analysis indicates that the major population comprising the BBFs is the new, earthward-going energetic ions that extend from ∼ 10 keV to MeV energies. We discuss below why $E \times B$ cannot account for the detailed features of the distribution function and energy spectra.

For the 1030 UT event, the $E \times B$ drift velocity is ∼200 km/s (the electric field inferred is $\sim 2mV/m$ in the dawn-to-dusk direction), whereas $\langle V_x \rangle$ reaches ∼600 km/s. For the 1430 UT event, the soft component (which appears in ∼ 20% of ∼ 50 events we have studied from the first 25 Wind perigee passes) does not have the same $V_\perp$ as the hard component, so there is no evidence for the $E \times B$ drift velocity (figure 2). Assuming the fluctuations seen in B is temporal, the $|\partial B/\partial t|$ and $|\partial^2 B/\partial t^2|$ obtained can reach $\sim 4nT/s$ and $\sim 6nT/s^2$. For scale lengths larger than the cyclotron radius of 1 keV protons in 10 nT field, these values yield a time-dependent electric field $> 1.6mV/m$ (which is larger than the typical dawn-dusk electric field of a few tenths of mV/m) and $|\partial E/\partial t| > 2.4mV/m/s$. Therefore, $E \times B$ drift cannot account for the large $\langle V_x \rangle$.

An important feature of the high velocity moment events in the CPS is that they involve enhancement of energetic ions. Typical energies of these ions are 10 keV, but significant ion flux increases occur to MeV energies. The ion energy spectra show directional dependence with ions > few keV to MeV from the tail representing the major contribution to the velocity moments. This is true for all of the events we have studied (∼50 events) which cover distances from ∼ 10-30 R_e in the tail. The observed energy spectra

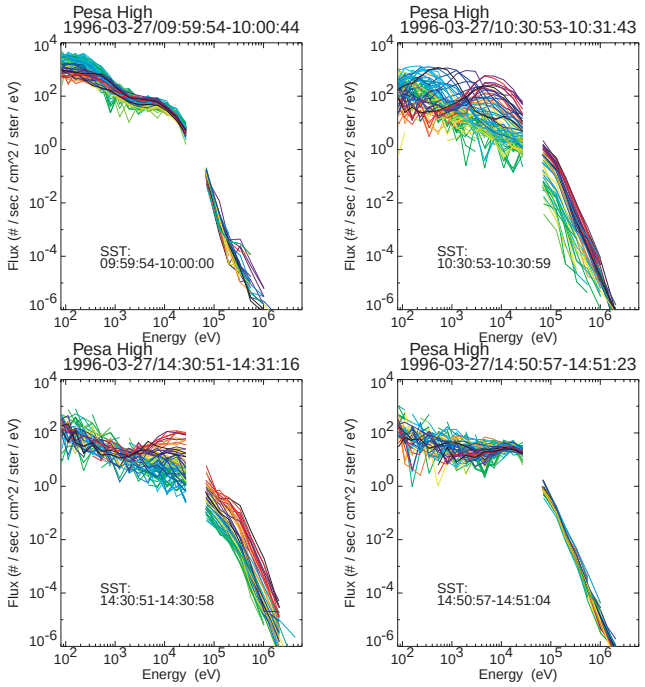

Figure 4. Energy spectra from ∼70 eV to several MeV before, during and after two sample BBF events. At 200 keV, there is ∼ 16% error due to counting statistics for the angular bin with the largest counts. ∼ 11% statistical error in the 2 MeV channel for the angular bin which has the largest counts.

during the BBF events cannot be obtained by any Galilean transformation (such as transforming to an $E \times B$ drift velocity frame) of the isotropic spectra. A comparison of 1430:51 and 1450:57 spectra shows that for $>$ 200 keV ions, the sunward fluxes of 1430:51 are about 2 orders of magnitude higher, but the tailward fluxes are comparable to the flux level of 1450:57.

The BBF events are closely associated with the tail current sheet reconfiguration. One normally observes the magnetic B_x component decreases dramatically just before a BBF event. The B_z component usually increases, but they are not the usual dipolarizations observed with substorm onsets since here they are accompanied by high frequency magnetic field oscillations in all three components. Moreover, the B_z values exceed what one would expect for the dipole field at that location, suggesting the current sheet disruption (Lui et al., 1992) alone cannot explain the results. (For the 1030 UT event, the dipole field is estimated as ≈ 4 nT, but the observed value exceeded 10 nT; for the 1430 UT event, the dipole estimate yields ≈ 6 nT, but $B_z \sim 15$ nT was observed.)

Examination of the relationship to substorms indicates the BBFs occur at all phases of a substorm (not shown). They have rarely been detected at the onset phase and some occur during weak auroral activities such as pseudo breakup events (Fillingim et al., 1999). For the events shown in Figure 1, they were observed ∼45 minutes (the 1030 UT event), and ∼5 minutes (the 1430 UT event) after the onsets. The high $\langle V_x \rangle$ BBF events are correlated with local intensification of the aurora and enhancement of the auroral kilometric radiation (AKR, not shown). The responsible mechanisms in the CPS are thus closely related to the unstable electron distributions which generate the AKR in the ionosphere. If the free energy of AKR comes from BBFs, another mechanism is required to operate at intermediate altitudes to convert the energy and momentum carried by ions to the electrons. Another possibility is that AKR and BBF are parallel phenomena, that is, they both are responses of the magnetosphere to some common external driving disturbance. To resolve whether AKR and BBF are causally related, a statistical timing analysis needs to be done. Future studies will examine the detailed plasma energy spectra to sort out adiabatic and nonadiabatic features to better identify the mechanisms involved in the CPS.

Acknowledgments. Research at the Universities of Washington and California at Berkeley is funded in part by NASA grants NAG5-3170 and NAG5-26580.

References

Angelopoulos, V., et al., Bursty bulk flows in the inner central plasma sheet , *J. Geophys. Res.*, *97*, 4027, 1992.

Angelopoulos, V., et al., Multipoint analysis of a bursty bulk flow event on April 11, 1985, *J. Geophys. Res.*, *101*, 4967, 1996.

Angelopoulos, V., et al., Magnetotail flow bursts: association to global magnetospheric circulation, relationship to ionospheric activity and direct evidence for localization, *Geophys. Res. Lett.*, *24*, 2271, 1997.

Chen, LiJen, et al., Multicomponent plasma distributions in the tail current sheet associated with substorms, *Geophys. Res. Lett.*, *27*, 843, 2000.

Fillingim, M., et al., Coincident Polar/UVI and Wind Observations of Pseudobreakups, accepted by *Geophys. Res. Lett.*, February, 2000.

Forbes, T. et al., Evidence for the tailward retreat of a magnetic neutral line in the magnetotail during substorm recovery, *Geophys. Res. Lett.*, *8*, 261, 1981.

Lin, R. P., et al., A three dimensional plasma and energetic particle investigation for the Wind spacecraft, *Space Sci. Rev.*, *71*, 125, 1995.

Lui, A. T. Y. et al., Current Disruption in the Near Earth Neutral Sheet., *J. Geophys. Res.*, *97*, 1461, 1992.

Parks, G. K., et al., New observations of ion beams in the plasma sheet boundary layer, *Geophys. Res. Lett.*, *25*, 3285, 1998.

Takahashi, K. and E. W. Hones, Jr., ISEE 1 and 2 observations of ion distributions at the plasma sheet-tail lobe boundary, *J. Geophys. Res.*, *93*, 8558, 1988.

D. Larson and R. P. Lin, Space Science Laboratory, University of California, Berkeley, CA 94720

Li-Jen Chen, M. McCarthy, and G. K. Parks, Geophysics Program, Box 351650, University of Washington, Seattle, WA 98195. (e-mail: lijen@u.washington.edu)

(Received December 21, 1999; revised March 31, 2000; accepted April 25, 2000.)